COBEM 2023 27TH INTERNATIONAL CONGRESS OF MECHANICAL ENGENEERING

ABCM Brazilian Society of Mechanical Sciences and Engineering
27th ABCM International Congress of Mechanical Engineering
December 04-08, 2023, Florianópolis-SC, Brazil

COB-2023-0635
PARAMETER IDENTIFICATION IN BIOHEAT TRANSFER MODELS USING THE TRANSITIONAL MARKOV CHAIN MONTE CARLO METHOD

Eduardo Cunha Classe[1]
eduardo.classe@iprj.uerj.br

Lucas da Silva Asth[1]
lucas.asth@iprj.uerj.br

Luiz Alberto da Silva Abreu[1]
luiz.abreu@iprj.uerj.br

Diego Campos Knupp[1]
diegoknupp@iprj.uerj.br

Leonardo Tavares Stutz[1]
ltstutz@iprj.uerj.br

[1]Universidade do Estado do Rio de Janeiro - Instituto Politécnico.
Rua Bonfim Vila Amélia, Nova Friburgo, RJ - Brasil.

Abstract. *Accurately estimating the unknown parameters in bioheat transfer is essential for numerous biomedical applications such as hyperthermia treatment, thermal imaging, and cryopreservation. In this work, the Transition Markov Chain Monte Carlo method (TMCMC) was applied for estimating the posterior distributions of certain parameters that can inform whether a region is healthy or likely to have tumor cells within the bioheat transfer. The TMCMC algorithm is a more recent approach that utilizes a series of transition kernels applied to the probability density function in steps. This results in better convergence and a higher likelihood of finding global minima. Furthermore, it is capable of evaluating the model evidence as a by-product, unlike the Markov Chains Monte Carlo method (MCMC), already well known in the literature. In this research, a non-linear bioheat transfer model will be used for the blood perfusion term (quadratically dependent on temperature) to simulate the measurement data of the direct problem. From these data, the posterior distributions of the unknown parameters will be estimated using the TMCMC, but now simpler models will be analyzed, including a constante model and a linear model with the perfusion term linearly dependent on temperature. The results obtained for the linear model have much less model evidence than for the model with the constant perfusion term, although in both models it is possible to identify (or not) the presence of tumors.*

Keywords: *Bayesian Methods, Bioheat Transfer, Inverse Problem, Model Evidence, TMCMC*

1. INTRODUCTION

The inverse problem involves determining unknown properties through indirect measurements (Orlande, 2012). These problems are often ill-posed, lacking a unique or stable solution. Small errors in input data or measurement noise can result in significant deviations in estimated parameters or boundary conditions (Parwani *et al.*, 2015; Orlande, 2012).

Inverse heat transfer problems pose additional challenges, including nonlinearity, leading to multiple local minima; insufficient and noisy data, exacerbating ill-posedness; computational complexity, being computationally intensive and time-consuming; and model uncertainty, where discrepancies or uncertainties in model assumptions can lead to errors in estimated parameters or boundary conditions (Ozisik *et al.*, 2002; Kaipio and Somersalo, 2006).

Various approaches exist to solve inverse problems, depending on the problem and available data. One common approach relates the parameter or function to be estimated to the performed measurements. However, this is not always feasible, and even when it is, the solution can be challenging. Different techniques, such as deterministic methods (Liu and Ozisik, 1996), stochastic methods (Kaipio and Fox, 2011), or neural networks (Jardim *et al.*, 2022), each have their advantages and limitations. In this work, a Bayesian inference approach will be adopted.

Bayesian inference offers advantages, including the ability to incorporate prior information and specialized knowledge, enhancing result interpretation and reducing uncertainty in parameter estimation (Kaipio and Fox, 2011). It provides a ro-

bust probabilistic framework, enabling the evaluation of uncertainties associated with estimates, presenting confidence intervals and probability distributions for inferred parameters (Orlande, 2012). This approach is flexible, handling problems with incomplete or noisy data, allowing for iterative and adaptive approaches with updates as new data are incorporated.

In heat transfer, inverse problems find applications in bioheat transfer ((Rojczyk *et al.*, 2017)), where estimating physical properties of the human body aids in diagnosing healthy or tumor tissue. Despite challenges, such as those discussed by Rojczyk *et al.*, there are advancements in methods like the TMCMC for tumor identification using dynamic thermography data.

Existing models for heat transfer in biological tissues face challenges due to small temperature ranges and the approximation of parameters as functions of temperature (Rossmann and Haemmerich, 2014). The choice of models depends on the study location in the human body. The model proposed by Iljaž *et al.* (2019) stands out for its good approximation to real data (Barros, 2022) and simplicity similar to the Pennes model, making it suitable for the present work.

Considering the high computational cost of the chosen model, evaluation of two simpler models to estimate parameters related to blood perfusion, with uniform coefficients throughout the layers (Cotta *et al.*, 2010), and metabolic heat generation rate will be explored for different data, aiming to differentiate them.

2. MATHEMATICAL FORMULATION FOR DIRECT PROBLEM

The problem under analysis was adapted from (Barros, 2022) and is defined by the following set of equations:

$$w(x)\frac{\partial T}{\partial t} = \frac{\partial T}{\partial x}\left[k(x)\frac{\partial T}{\partial x}\right] + P(x,T) \qquad in \quad 0 < x < L \qquad for \quad t > 0 \tag{1}$$

$$T(x,t) = T_E(x) \qquad in \quad 0 < x < L \qquad for \quad t = 0 \tag{2}$$

$$-k(x)\frac{\partial T}{\partial x} = h(T_\infty - T) \qquad in \quad x = 0 \qquad for \quad t > 0 \tag{3}$$

$$\frac{\partial T}{\partial x} = 0 \qquad in \quad x = L \qquad for \quad t > 0 \tag{4}$$

Where $w(x)$ is the thermal capacity of the fabric, $k(x)$ is the thermal conductivity of the fabric, $P(x,T)$ is the source term, L is the total thickness of the skin, $T_E(x)$ is the stationary solution, T_∞ is the ambient temperature and h is the convective heat transfer coefficient. The thermal capacity and the source term are represented by:

$$w(x) = \rho(x)c_p(x) \tag{5}$$

$$P(x,T) = \omega(x,T)\rho_b c_b(T_a - T) + q_m \tag{6}$$

And here, $\rho(x)$ is the specific mass of the tissue, $c_p(x)$ is the specific heat of the tissue, $\omega(x,T)$ is the term related to blood perfusion, ρ_b is the specific mass of blood, c_b is the specific heat of blood, T_a is the temperature of arterial blood and q_m is the generation of metabolic heat. The problem under analysis has four layers, the outermost surface is the epidermis, followed by the dermis, subcutaneous tissue and internal tissue where the properties vary according to each layer.

The direct problem is solved in order to simulate measurements carried out by dynamic thermography on a surface on which information is desired regarding the existence (or not) of superficial tumors. Dynamic thermography is simulated so that there is cooling on the external surface in perfect contact with a thermal reservoir at 0°C for 30 seconds, and then measurements are carried out so that the external surface exchanges heat by convection at room temperature.

3. METHODOLOGY FOR SOLVING THE INVERSE PROBLEM

In this work, the Transitional Markov Chain Monte Carlo method will be used, as previously mentioned this method utilizes the Bayesian approach. The main advantages of this approach is that, by using probability, its methods do not estimate a single value, but a region in which the parameter of interest may be, indicating the probability of each point within that region as well as the most likely point, and it is possible still use prior knowledge about that parameter to estimate that parameter.

In general, the methods within the Bayesian approach: (i) use prior knowledge of the information to be estimated to represent an *priori* distribution $\pi(P)$; (ii) appropriately select a likelihood distribution $\pi(Y|P)$ that models the measurement errors; and (iii) develops methods to explore the *posterior* distribution (Orlande, 2015). The methods use the Bayes theorem to estimate the posterior distribution. Equation (7) represents Bayes' theorem without the marginal probability density of measurements, which in addition to being difficult to calculate plays the role of a normalizing constant.

$$\pi(\mathbf{P}|\mathbf{Y}) \propto \pi(\mathbf{Y}|\mathbf{P})\pi(\mathbf{P}) \tag{7}$$

3.1 Transitional Markov Chain Monte Carlo (TMCMC)

The Transitional Markov Chain Monte Carlo (TMCMC) method was proposed by Ching and Chen (2007) and tries to avoid direct sampling of the *posteriori* distribution. This method starts with independent samples of an *a priori* distribution. In the following steps, the sampling distribution is gradually transformed so that it approaches the *a posteriori* distribution. This way Eq. (7) is modified to:

$$\pi_j(\mathbf{P}|\mathbf{Y}) \propto \pi(\mathbf{P})\pi(\mathbf{Y}|\mathbf{P})^{p_j} \qquad j = 0, 1, ..., m \qquad 0 = p_0 < p_1 < ... < p_m = 1 \tag{8}$$

Where the index j denotes the stage number. It is easy to note that $\pi_0(\mathbf{P}|\mathbf{Y})$ is the prior distribution and $\pi_m(\mathbf{P}|\mathbf{Y})$ is the posterior itself. The steps for the TMCMC algorithm are described below (Ching and Wang, 2016):

1. Get samples $\{\mathbf{P}_{0,1}, \mathbf{P}_{0,2}, ..., \mathbf{P}_{0,N}\}$ from priori $f_0(\mathbf{P}) = \pi(\mathbf{P})$ using Monte Carlo simulation. Let $p_0 = 0$. Repeat steps 2 and 3 for $j = \{0, 1, 2, ...\}$.

2. Calculate the likelihood distributions $\{\pi(\mathbf{Y}|\mathbf{P}_{j,1}), ..., \pi(\mathbf{Y}|\mathbf{P}_{j,N})\}$ and calculate $w_{j,k} = \pi(\mathbf{Y}|\mathbf{P}_{j,k})^{p_{j+1}-p_j}$. Note that p_{j+1} must be chosen so that the COV of the importance weights $\{w_{j,1}, ..., w_{j,N}\}$ are equal to 100%. Also calculate the normalized weights $\{\bar{w}_{j,1}, ..., \bar{w}_{j,N}\}$.

3. According to the normalized weights $\{\bar{w}_{j,1}, ..., \bar{w}_{j,N}\}$, choose candidates randomly from $\{ mathbf P_{j,1}, \mathbf{P}_{j,2}, ..., \mathbf{P}_{j,N}\}$, propose a new candidate according to the distribution $N(\mathbf{P}_{j,k}, \Sigma_j)$ and form the sequence $\{\mathbf{P}_{j+1,1}, \mathbf{P}_{j+1,2}, ..., \mathbf{P}_{j+1}\}$. The covariance matrix Σ_j is described by Eq. (9).

$$\Sigma_j = \beta^2 \sum_{k=1}^{N_j} w_{j,k} \left[\left(\mathbf{P}_{j,k} - \frac{\sum_{l=1}^{N_j} w_{j,l} \cdot \mathbf{P}_{j,l}}{\sum_{l=1}^{N_j} w_{j,l}} \right) \times \left(\mathbf{P}_{j,k} - \frac{\sum_{l=1}^{N_j} w_{j,l} \cdot \mathbf{P}_{j,l}}{\sum_{l=1}^{N_j} w_{j,l}} \right) \right]^T \tag{9}$$

The entire algorithm can be found in Ching and Chen (2007).

4. DISCUSSION AND RESULTS

The values of the parameters used in solving the direct problem in Eq. (1 - 4) are shown in Tab. 1 to Tab. 3 below. It is noteworthy here that measurements are generated for two cases, the first case is when the tissue is healthy and the other is when the tissue is tumor.

Table 1: Layer properties

Camada	$\rho(\mathbf{kg/m^3})$	$\mathbf{c_p(J/kgK)}$	$\mathbf{k(W/mK)}$	$\mathbf{L(m)}$
Epidermis	1030	3852	0.558	0.00044
Dermis	1200	3300	0.45	0.00164
Subcutaneous Tissue	1000	2500	0.19	0.01
Inner Tissue	1000	4000	0.50	0.03

Tab. 1 shows the thermophysical properties of each layer, it is important to highlight that the functions of each property were smoothed according to the following equation:

$$\Theta(x) = \sum_{n=1}^{N_s} \Theta_{n-1} + (\Theta_n - \Theta_{n-1})\, \delta_n(x) \tag{10}$$

$$\delta_n(x) = \left[1 + e^{-200(x-x_m)/L}\right]^{-1} \qquad x_m \in [0, L] \tag{11}$$

Where N_s is the number of smoothing functions, x_n is the n-th transition position between two adjacent fabric layers, n is the n-th thermal properties tuning parameter and L is the total thickness of the tissue. Table 2 shows other parameters used to solve the inverse problem, where different values are observed for the rate of metabolic heat generation in healthy tissues and tissues with the presence of tumors. Furthermore, two parameters related to blood perfusion are noted, which is described as follows for the healthy case:

$$\omega(x, T) = aT + b \qquad 0 < x < L \tag{12}$$

Table 2: General parameters for solving the direct problem

Parameter	**Value**
Specific heat of blood (c_b)	3770 J/kgK
Blood Density (ρ_b)	1060 kg/m^3
Arterial blood temperature (T_a)	37 C
Heat transfer coefficient (h)	10 W/m^2K
Ambient temperature (T_∞)	20 C
Total cooling time ($t_{f,c}$)	30 s
Total measurement time (t_f)	600 s
Healthy tissue metabolic heat generation rate ($q_{m,h}$)	420 W/m^3
Tumor tissue metabolic heat generation rate ($q_{m,t}$)	3680 W/m^3
Angular parameter for blood perfusion term in healthy tissue (a)	3.6×10^{-5}
Linear parameter for blood perfusion term in healthy tissue (b)	9.6×10^{-5}

Table 3: Blood perfusion term parameter for tumor tissue

Parameter	**Epidermis**	**Dermis**	**SubcutaneousTissue**	**InnerTissue**
a	0.0	0.27×10^{-5}	0.86888×10^{-7}	0.2346×10^{-5}
b	0.0	0.29×10^{-4}	-0.79453×10^{-6}	-0.21452×10^{-4}
c	0.0	0.15×10^{-2}	0.11294×10^{-4}	0.30495×10^{-3}

And finally, Tab. 3 shows the values related to the blood perfusion term used to solve the problem directly for the tumor case. Each layer has a function quadratically dependent on temperature as described in Eq. (13), and smoothing between layers is done as shown by Eq. (10).

$$\omega(x,T) = aT^2 + bT + c \qquad 0 < x < L \tag{13}$$

Fig. 1 shows the data obtained by solving the direct problem for each of the cases, with a standard deviation of measurement errors of $0.2°C$ and a total of 151 measurements. It can be seen from the graphical analysis that the measurements differ slightly over time. Tumor tissue is heated faster than healthy tissue.

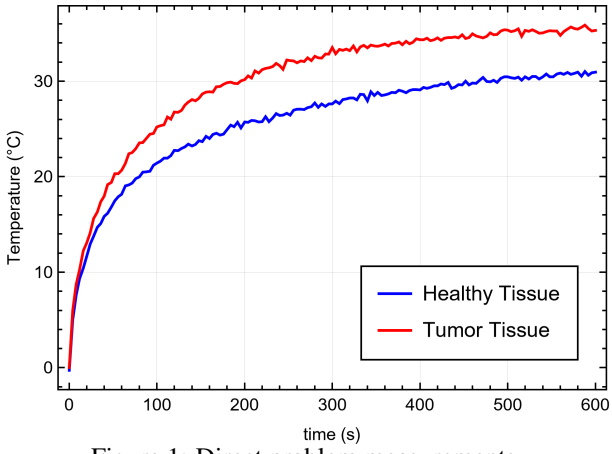

Figure 1: Direct problem measurements.

The objective of this work is to explore the application of the TMCMC method to identify tumors, and the most sensitive parameter to the presence of this malignant cell is blood perfusion, as observed in Rojczyk *et al.* (2017), although other parameters also have their values changed. In this work, only blood perfusion and metabolic heat transfer rate are changed to differentiate cases, so the objective of the inverse problem is to identify distinct values for these two properties.

However, the model used to solve the direct problem is very computationally expensive, especially the quadratic model used for tumor tissue, so it will be used a linear model and a constant model, with uniform coefficients throughout the layers (Cotta *et al.*, 2010), described by Eq. (12) and Eq. (14) respectively. Furthermore, although Bayesian methods have proven to be good for estimating functions, as seen in (Abreu *et al.*, 2022), an average parameters related to the blood perfusion will be used for all layers.

$$\omega(x,T) = \omega \qquad 0 < x < L \tag{14}$$

4.1 Constant model

A total of 1000 samples were used, $\beta = 0.2$ and it was considered that $0 \leq \omega \leq 0.5$ and $0 \leq q_m \leq 5000$. The average execution time of the algorithm for both cases was approximately 17 minutes and the estimated results are presented in Tab. 4 below.

Table 4: Values estimated with the constant model

Parameter	**HealthyTissue**		**TumorTissue**	
	Estimated value	Standard deviation	Estimated value	Standard deviation
ω	0.001178	0.000054	0.006709	0.000083
q_m	2244.46	1539.13	4039.95	951.83

The histograms are presented in Fig. 2 below. The first two figures show the results for the healthy case and the other two for the tumor case.

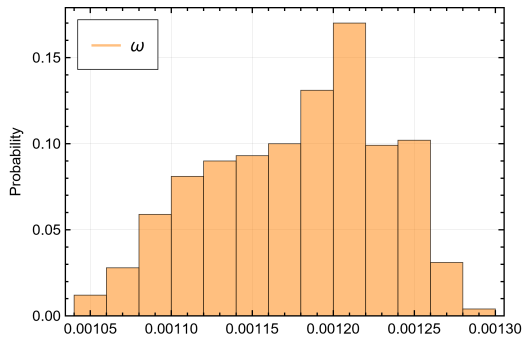

(a) Parameter ω for healthy measurements

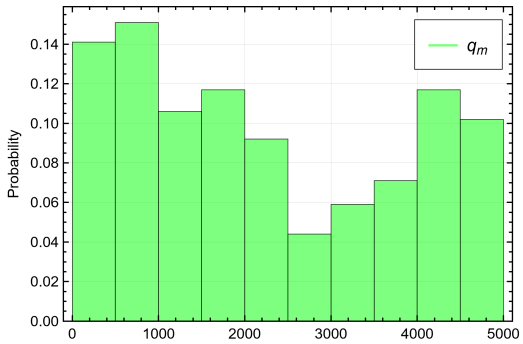

(b) Parameter q_m for healthy measurements

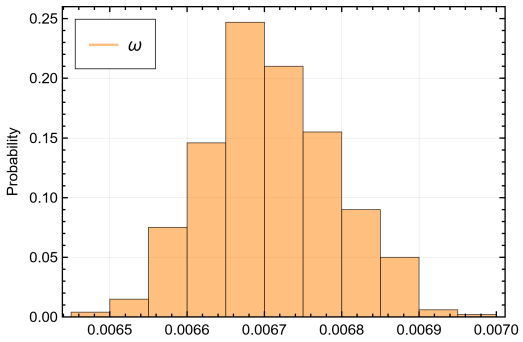

(c) Parameter ω for tumor measurements

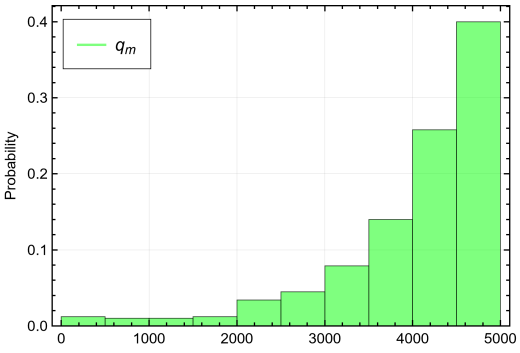

(d) Parameter q_m for tumor measurement

Figure 2: Histograms of estimated results for constant model

By analyzing the images presented, it is noted that the estimated values for the blood perfusion parameter differ significantly, for the tumor case the value is approximately 5.7 times higher than for the healthy case. Furthermore, a preferential region can be seen for the estimated data of the q_m parameter for the tumor case, although the comparison between both images cannot differentiate the two cases.

The estimated values were used to solve the direct problem by the same constant model in order to compare with the measurements, these comparisons are shown in Fig. 3 below along with their respective 95% confidence intervals. Furthermore, the root-mean-square deviation of the problem for the measurements of the healthy case was 24.3% and for the tumor case it was 30.7%.

By analyzing Fig. 3, a good fit is observed between the measurements of the direct problem and the measurements of the estimated parameters, in addition, a very narrow confidence band is noted.

4.2 Tumour tissue

In the same way as for healthy tissue, the results for tumor tissue are presented here. A total of 100 samples were used, due to the large computational cost, $\beta = 0.2$ and it was considered that $0 \leq a \leq 0.5 \times 10^{-2}$, $0 \leq b \leq 0.5 \times 10^{-2}$ and

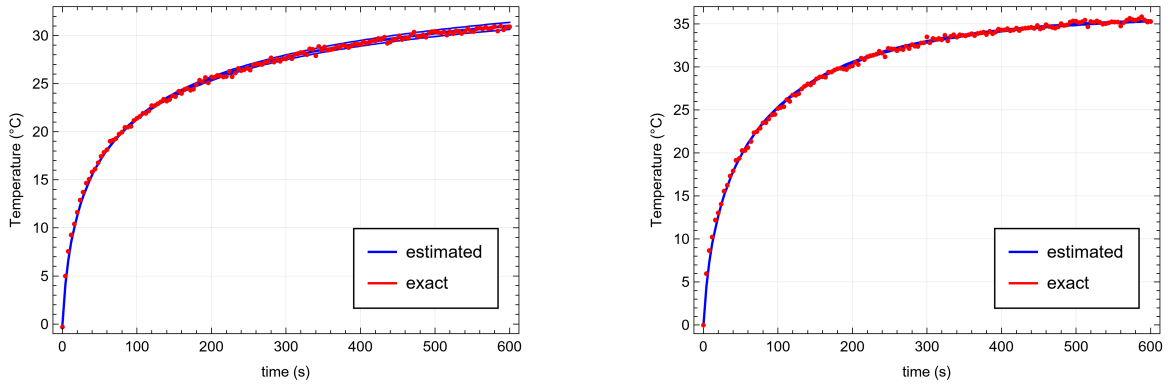

(a) Healthy case (b) Tumor case

Figure 3: Comparison between measurements and confidence interval for the constant model

$0 \leq q_m \leq 5000$. The average execution time of the algorithm for both cases was approximately 256 minutes (15 times longer than the constant model, and with 10 times fewer samples) and the estimated results are presented in Tab. 5 below.

Table 5: Values estimated with the linear model

Parameter	**HealthyTissue**		**TumorTissue**	
	Estimated value	Standard deviation	Estimated value	Standard deviation
a	-0.000078	0.000004	0.000018	0.000002
b	0.003288	0.000114	0.003985	0.000044
q_m	1613.24	216.116	3964.16	546.134

The histogram of the parameter q_m is shown in Fig. 4 and the estimated blood perfusion curves for both cases with their respective 95% confidence intervals are shown in Fig. 5.

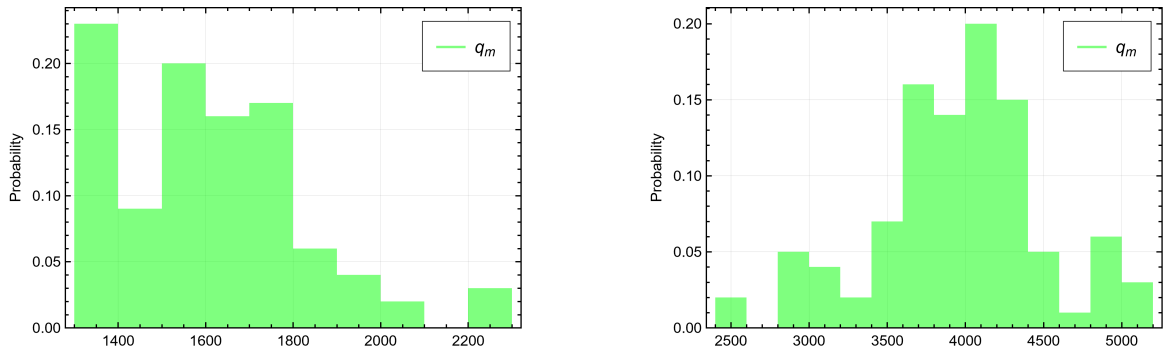

(a) Healthy case (b) Tumor case

Figure 4: Histogram of the q_m parameter estimated for both cases

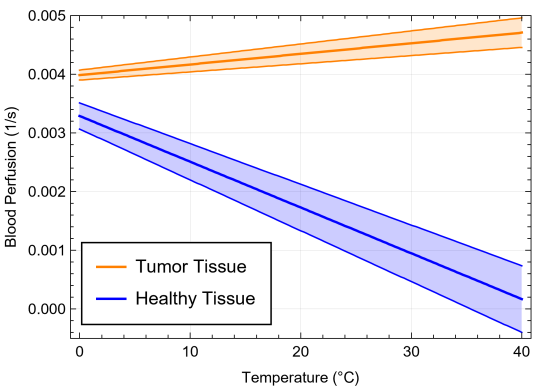

Figure 5: Estimated blood perfusion $\omega(T)$

It can be noted that the estimates of both parameters differ significantly. The q_m parameter for the tumor case is around 2.5 times greater than that for the healthy case, and by analyzing Fig. 5 distinct curves for perfusion are observed in the analyzed temperature range.

Comparisons of estimated values with measurement data are shown in Fig. 6 along with their respective 95% confidence intervals. Where wider regions of reliability are noted than for the constant model, this is due to the fact that fewer samples were used than in the other case.. Furthermore, the root-mean-square deviation of the problem for the measurements of the healthy case was 30.0% and for the tumor case it was 49.4%.

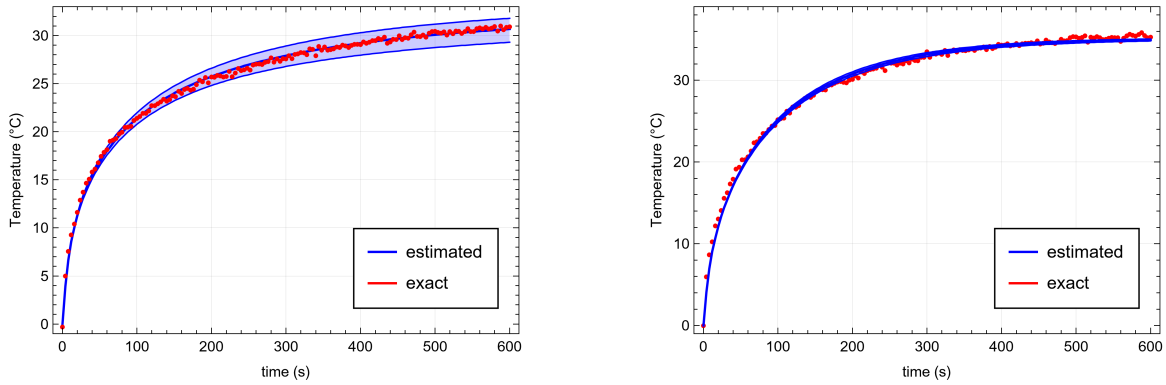

(a) Healthy case (b) Tumor case

Figure 6: Comparison between measurements and confidence interval for the linear model

After obtaining the results, the model evidence from the last stages was analyzed in order to choose the most likely model to be used, and for the two cases analyzed the model evidence for the linear model was approximately 100% count 0% of constant model.

5. CONCLUSION

The model evidence indicates that the model that comes closest to the model used in the direct problem is the linear model, and this is due to the fact that this model is closer to the quadratic model than the constant model for the tumor case, and because it is the same model for the healthy case. However, there is a high computational cost to solve the inverse problem when using the linear model, as we can see from the difference in the average execution time between each model, around 15 times greater for the linear model and using 10 times fewer samples, which which makes the reliability interval larger.

However, when analyzing the histograms and the estimated results, it can be stated that both models used can inform us about the presence or absence of tumors, since the regions in which the samples are arranged differ from each other. Furthermore, the results obtained show that simpler models can be used to identify tumors, and the TMCMC method can be used to validate (or even propose) new models related to bioheat transfer through analysis of model evidence.

6. ACKNOWLEDGEMENTS

This study was financed in part by the Coordenação de Aperfeiçoamento de Pessoal de Nível Superior - Brasil (CAPES) - Finance Code 001.

In addition, it was supported by Conselho Nacional de Desenvolvimento Científico e Tecnológico (CNPq) and the Fundação Carlos Chagas Filho de Amparo à Pesquisa do Estado do Rio de Janeiro (FAPERJ).

7. REFERENCES

Abreu, L.A.S., Guedes, G.A., Classe, E.C. and Knupp, D.C., 2022. "Estimativa do perfil de temperatura na entrada de dutos via método de monte carlo com cadeias de markov". *Revista Cereus*, Vol. 14, No. 4, pp. 129–143.

Barros, T.M.S.M., 2022. *Modelagem computacional de problemas de biotransferência de calor empregando transformações integrais, metamodelos e inferência Bayesiana*. Ph.D. thesis, Pós-Graduação em Modelagem Computacional, Instituto Politécnico, da Universidade do Estado do Rio de Janeiro, Nova Friburgo, Brasil.

Ching, J. and Chen, Y.C., 2007. "Transitional markov chain monte carlo method for bayesian model updating, model class selection, and model averaging". *Journal of engineering mechanics*, Vol. 133, No. 7, pp. 816–832.

Ching, J. and Wang, J.S., 2016. "Application of the transitional markov chain monte carlo algorithm to probabilistic site characterization". *Engineering Geology*, Vol. 203, pp. 151–167.

Cotta, R.M., Cotta, B.P., Naveira-Cotta, C.P. and Cotta-Pereira, G., 2010. "Hybrid integral transforms analysis of the bioheat equation with variable properties". *International journal of thermal sciences*, Vol. 49, No. 9, pp. 1510–1516.

Iljaž, J., Wrobel, L.C., Hriberšek, M. and Marn, J., 2019. "Numerical modelling of skin tumour tissue with temperature-dependent properties for dynamic thermography". *Computers in Biology and Medicine*, Vol. 112, p. 103367.

Jardim, L., Knupp, D.C., Domingos, R.P., Abreu, L.A.S., Corona, C.C. and Silva Neto, A.J., 2022. "Contact failure identification in multilayered media via artificial neural networks and autoencoders". *Anais da Academia Brasileira de Ciências*, Vol. 94.

Kaipio, J. and Somersalo, E., 2006. *Statistical and computational inverse problems*, Vol. 160. Springer Science & Business Media.

Kaipio, J.P. and Fox, C., 2011. "The bayesian framework for inverse problems in heat transfer". *Heat Transfer Engineering*, Vol. 32, No. 9, pp. 718–753.

Liu, F. and Ozisik, M., 1996. "Estimation of inlet temperature profile in laminar duct flow". *Inverse Problems in engineering*, Vol. 3, No. 1-3, pp. 131–143.

Orlande, H.R., 2012. "Inverse problems in heat transfer: new trends on solution methodologies and applications". *Journal of Heat Transfer*, Vol. 134, No. 3.

Orlande, H.R., 2015. "The use of techniques within the bayesian framework of statistics for the solution of inverse problems". *Metti 6 Advanced School: Thermal Measurements and Inverse Techniques*.

Ozisik, M.N., Orlande, H.R. and Kassab, A., 2002. "Inverse heat transfer: fundamentals and applications". *Appl. Mech. Rev.*, Vol. 55, No. 1, pp. B18–B19.

Parwani, A.K., Talukdar, P. and Subbarao, P., 2015. "Estimation of boundary heat flux using experimental temperature data in turbulent forced convection flow". *Heat and mass Transfer*, Vol. 51, pp. 411–421.

Rojczyk, M., Orlande, H.R.B., Colaço, M.J., Szczygieł, I., Nowak, A.J., Białecki, R.A. and Ostrowski, Z., 2017. "Inverse heat transfer problems: an application to bioheat transfer". *Computer Assisted Methods in Engineering and Science*, Vol. 22, pp. 365–383.

Rossmann, C. and Haemmerich, D., 2014. "Review of temperature dependence of thermal properties, dielectric properties, and perfusion of biological tissues at hyperthermic and ablation temperatures". *Critical Reviews™ in Biomedical Engineering*, Vol. 42, No. 6.

8. RESPONSIBILITY NOTICE

The authors are solely responsible for the printed material included in this paper.